JACS
JOURNAL OF THE AMERICAN CHEMICAL SOCIETY
Article
Cite This: J. Am. Chem. Soc. 2019, 141, 4119−4129
pubs.acs.org/JACS

Anion Recognition in Water by Charge-Neutral Halogen and Chalcogen Bonding Foldamer Receptors

Arseni Borissov,[†] Igor Marques,[‡] Jason Y. C. Lim,[†,§] Vítor Félix,[‡] Martin D. Smith,[†] and Paul D. Beer*[,†]

[†]Chemistry Research Laboratory, Department of Chemistry, University of Oxford, Mansfield Road, Oxford OX1 3TA, U.K.
[‡]Department of Chemistry, CICECO - Aveiro Institute of Materials, University of Aveiro, 3810-193 Aveiro, Portugal

Supporting Information

ABSTRACT: A novel strategy for the recognition of anions in water using charge-neutral σ-hole halogen and chalcogen bonding acyclic hosts is demonstrated for the first time. Exploiting the intrinsic hydrophobicity of halogen and chalcogen bond donor atoms integrated into a foldamer structural molecular framework containing hydrophilic functionalities, a series of water-soluble receptors was constructed for an anion recognition investigation. Isothermal titration calorimetry (ITC) binding studies with a range of anions revealed the receptors to display very strong and selective binding of large, weakly hydrated anions such as I^- and ReO_4^-. This is achieved through the formation of 2:1 host−guest stoichiometric complex assemblies, resulting in an encapsulated anion stabilized by cooperative, multidentate, convergent σ-hole donors, as shown by molecular dynamics simulations carried out in water. Importantly, the combination of multiple σ-hole−anion interactions and hydrophobic collapse results in I^- affinities in water that exceed all known σ-hole receptors, including cationic systems (β_2 up to 1.68×10^{11} M^{-2}). Furthermore, the anion binding affinities and selectivity trends of the first example of an all-chalcogen bonding anion receptor in pure water are compared with halogen bonding and hydrogen bonding receptor analogues. These results further advance and establish halogen and chalcogen bond donor functions as new tools for overcoming the challenging goal of anion recognition in pure water.

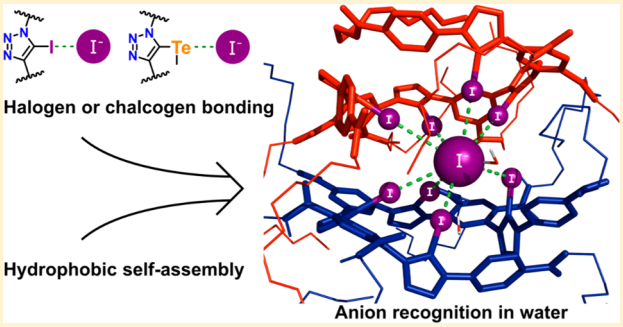

INTRODUCTION

One of the key challenges in modern anion supramolecular chemistry is the recognition of anions in water, which needs to be achieved for applications in biology, healthcare, and environmental monitoring under aqueous conditions to be realized. To date, an overwhelming majority of reported abiotic anion receptors operate in organic solvents, whose lower polarity compared to that of water facilitates anion coordination via noncovalent interactions such as hydrogen bonding (HB) and anion−π interactions.[1] In water, the recognition of anions is thwarted by their strong hydration, resulting in an additional energetic barrier due to desolvation during host−guest binding. Early examples of anion binding in water were dominated by highly charged polycationic receptors to enhance the electrostatic attraction with anions.[2−8] More recent years have offered alternative strategies, such as the formation of strong coordinate bonds with Lewis acidic main group elements (e.g., Sb),[9,10] transition metals,[11−14] and lanthanides.[15−17] Counterintuitively, low charge or neutral receptors have also recently been demonstrated to be capable of functioning in aqueous media.[18] Notable rare examples that operate in 100% water include cyclopeptide macrocycles,[19,20] bambus[6]urils,[21,22] biotin[6]urils,[23,24] and indolocarbazoles,[25] where hydrogen bonding and hydrophobic effects contribute to the preferential recognition of weakly hydrated chaotropic anions (e.g., PF_6^-, SCN^-, and ClO_4^-).

The applications of σ-hole interactions such as halogen bonding (XB) and chalcogen bonding (ChB), the attractive supramolecular interactions between heavy electron-deficient group 17/16 atoms and Lewis bases[26,27] are important recent developments in the field. Compared to HB, these interactions are characterized by more stringent directionality and greater hydrophobicity and are less sensitive to solvent and pH changes.[28−30] Recent advances in the use of XB and ChB[28,31] include several types of anion receptors,[32−35] self-assembled structures,[36−39] and transmembrane anion transporters.[40−43] Applications in aqueous solution are, however, extremely rare and based exclusively on cationic receptors. These include the observation of helicate complexes between I^- and iodopyridinium receptors[44,45] as well as our work on achieving anion recognition in water for XB[46−48] and aqueous−organic media for ChB[49] using macrocyclic and mechanically interlocked hosts. Most importantly, these σ-hole donor hosts often outperform HB host analogues in binding affinities and offer greatly contrasting anion selectivity. Nonetheless, the resulting

Received: January 5, 2019
Published: February 7, 2019

DOI: 10.1021/jacs.9b00148
J. Am. Chem. Soc. 2019, 141, 4119−4129

anion affinities still pale in comparison to natural biotic receptors.

Herein, we present a novel strategy for aqueous anion binding by σ-hole donor hosts, which capitalizes on the tendency of XB and ChB donor atoms (I/Te) to self-assemble in water due to their intrinsic hydrophobicity. The confinement of these hydrophobic functions within a shielded core of a folded receptor can create a stabilized anion binding cavity with multiple σ-holes directed in a convergent manner. This process, which drives the folding of peptides into complex tertiary and quaternary structures, has successfully been exploited by Flood and co-workers, who used a preorganized aryl-triazole HB foldamer receptor to bind Cl^- and $H_2PO_4^-$ in 1:1 MeCN/H_2O solution via C−H hydrogen bond donors in a dehydrated microenvironment.[50,51] By combining the strict geometric control of σ-hole interactions with receptor folding via hydrophobic collapse, we present the first-ever series of charge-neutral XB and ChB receptors (Figure 1) capable of very strong and highly selective I^- binding in pure water. Reinforced by the tendency of hydrophobic σ-hole donors to converge, the resulting I^- affinities surpass all known cationic XB receptors, even exceeding the I^- affinity of the natural Na^+/I^- symporter (NIS) protein in the Na^+-bound form.[52] Furthermore, the first example of an all-ChB anion receptor studied in pure water allows a direct anion binding affinity and selectivity trend comparison with XB and HB receptor analogues.

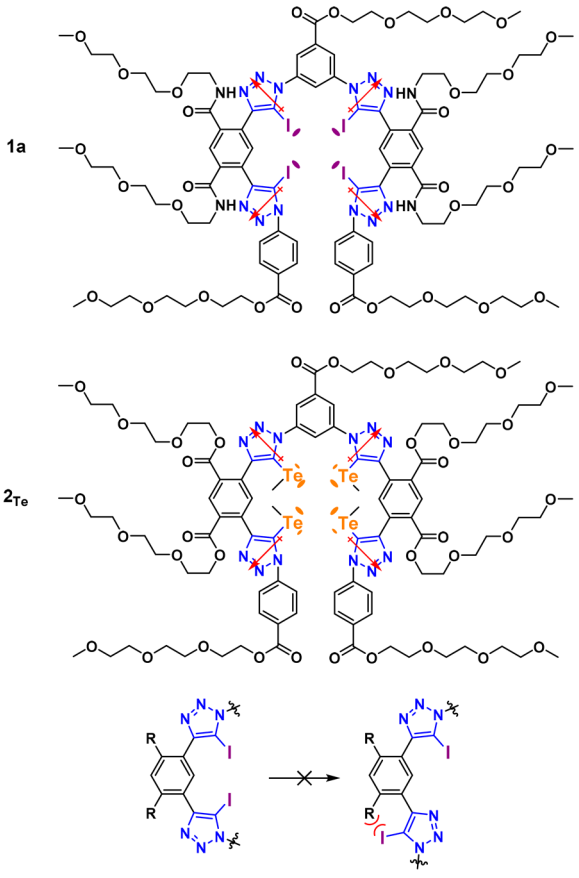

Figure 1. Structures of XB and ChB anion receptors described in this work. Local dipoles of the triazole units and positions of σ-holes are highlighted. (Bottom) Preorganization of receptor arms by restricted intramolecular rotation.

RESULTS AND DISCUSSION

Receptor Design and Synthesis. Building upon our previous work on tetradentate iodotriazole XB receptors,[53] we designed a foldamer structure consisting of alternating 5-iodo- or 5-methyltellanyl triazoles and 1,3-phenylene units while carrying several amide- or ester-bound tri(ethylene glycol) groups to impart water solubility (Figure 1). The positioning of solubilizing groups ortho to the I/MeTe-triazoles sterically restricts the relative rotation of triazole and phenylene units. As the bulky I or Te atoms cannot move past the ortho substituent, the arms of the receptor are preorganized toward a folded state, which is favorable to anion binding. The host molecules are also clearly differentiated into a hydrophilic outer rim and a hydrophobic interior to stabilize folded conformations that contain a central cavity lined with σ-hole donors. Groups at the termini of the receptor can be varied (Scheme 1) to customize the binding and sensing properties. For instance, the appendage of 4-aminonaphthaleneimide fluorophores to the XB receptor scaffold enabled significant "turn on" fluorescent I^- sensing (vide infra).

The tetrakis(iodotriazole) framework of XB receptors **1a−d** was assembled in a sequence of copper(I)-catalyzed azide−alkyne cycloaddition (CuAAC) reactions (Scheme 1).[54] First, azide terminal synthon **5a,c,d** was reacted with bis(iodoethynyl) precursor **7** in a statistical reaction leading to arm fragment **3**. In the case of azide **5b**, the steric bulk of its naphthaleneimide unit prevented it from reacting with **7** under the usual CuAAC conditions. Target iodotriazole **3b** was instead synthesized from **5b** and **6** in a one-pot desilylation−cycloaddition−iodination procedure. (See the SI for details.) In this method, cycloaddition occurs between the azide and Cu alkynide, thus circumventing the steric restrictions. Arm fragments **3a−d** were then joined with bis(azide) core synthon **8**. Finally, resulting precursors **4a−d** were treated with primary amine **9**. This provided final products **1a−d** via amidation of the labile ethylparaben esters in **4a−d**. Following TMS deprotection of **6**, a similar sequence of CuAAC and amidation steps provided HB analog $\mathbf{1a_H}$. The introduction of tri(ethylene glycol) amide groups in the last step avoids the terminal iodination of alkynes in the vicinity of amides, which tends to provide cyclized products instead of the desired iodoalkynes.[55,56] Additionally, this alleviates the purification difficulties common to heavily PEG-substituted compounds.

Water-soluble ChB anion receptor $\mathbf{2_{Te}}$ was derived from bis(methyltellanylethynyl) precursor $\mathbf{11_{Te}}$ in two CuAAC steps,[57] analogous to the synthesis of **1a−d** (Scheme 2). To prepare $\mathbf{11_{Te}}$, a transmetalation between Ag alkynide and MeTeBr[58] was performed, which formed $\mathbf{11_{Te}}$ under very mild conditions and in high yield. To the best of our knowledge, this is an entirely new method of accessing organotellanyl alkynes. In $\mathbf{2_{Te}}$, an all-ester scaffold was used, replacing the amide linkers present in **1a−d** with ester groups. This was due to synthesis difficulties which prevented the clean amidation of ethylparaben esters in the presence of 5-(methyltellanyl) triazoles as well as the formation of MeTe-alkynes in the vicinity of the amides.

To attain a precise comparison between ChB and XB anion receptors, an all-ester XB compound $\mathbf{2_I}$ was also prepared via an analogous route. As the all-ester backbone is less hydrophilic than the ester−amide type present in **1a−d**, receptors $\mathbf{2_{Te}}$ and $\mathbf{2_I}$ displayed much lower water solubility. Interestingly, their solubility sharply decreased with increasing temperature. This

DOI: 10.1021/jacs.9b00148
J. Am. Chem. Soc. 2019, 141, 4119−4129

Scheme 1. Synthesis of XB Anion Receptors 1a–d and HB Analog $1a_H$

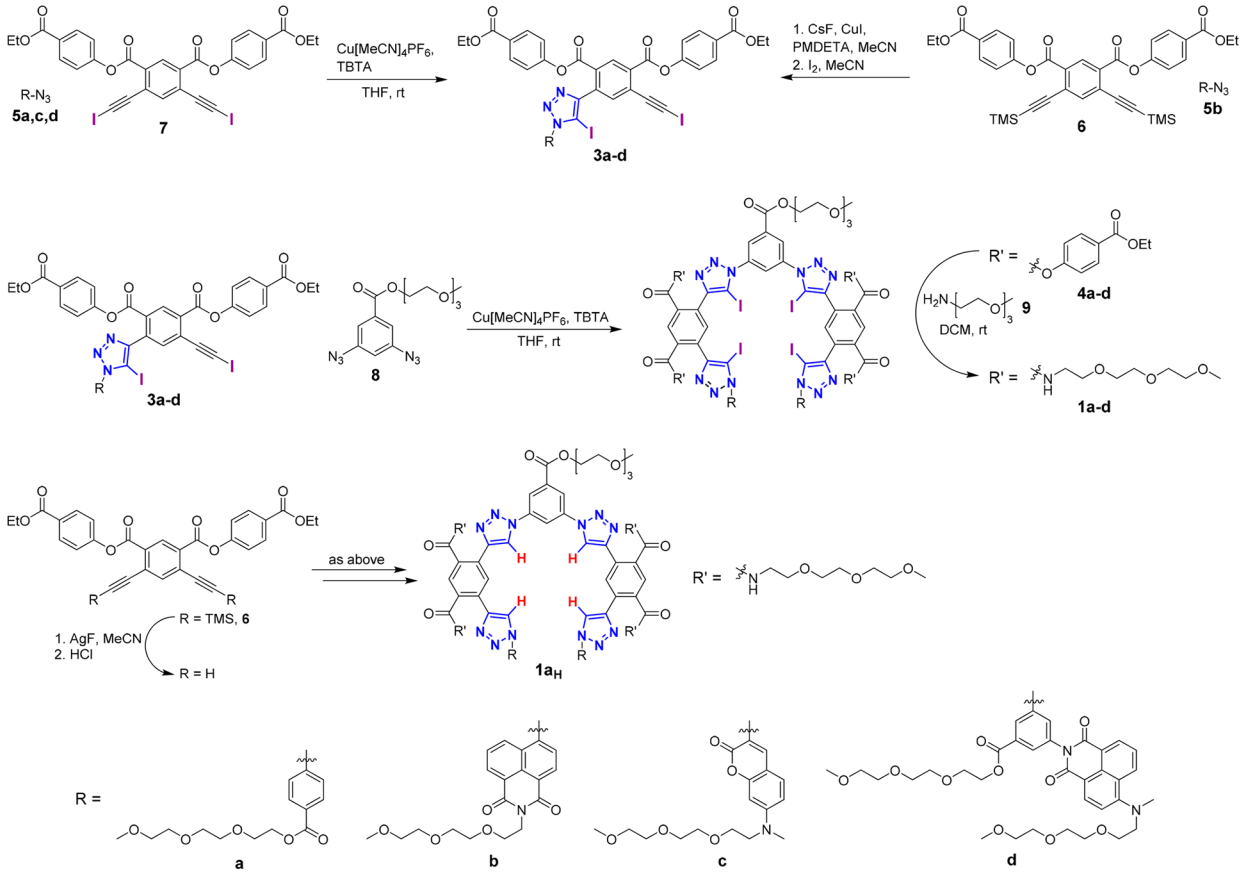

Scheme 2. Synthesis of Tri(Ethylene glycol) Ester-Substituted Bis(Methyltellanylethynyl) and Bis(Iodoethynyl) Precursors 11_{Te} and 11_I That Allow Access to ChB Anion Receptor 2_{Te} and Its XB Analog 2_I via CuAAC Sequences Similar to Those Shown in Scheme 1

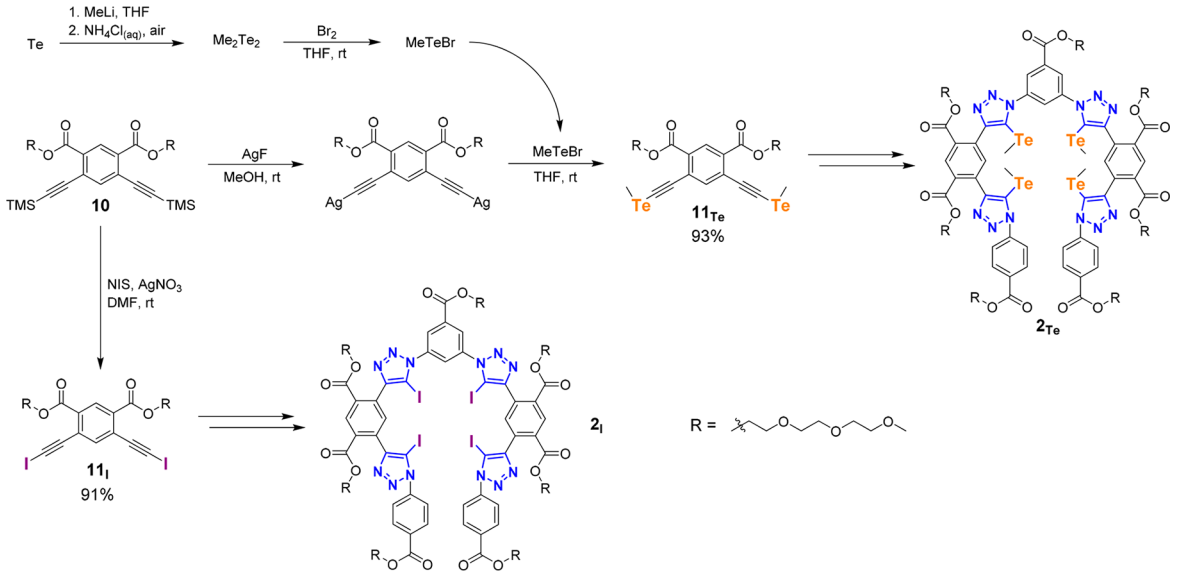

effect can be attributed to the transition of tri(ethylene glycol) chains from C–C gauche to the less hydrophilic anti conformation.[59,60]

Anion Binding Studies. The anion binding properties of all receptors **1a–d**, $1a_H$, 2_{Te}, and 2_I were investigated in water by ITC. All experiments with **1a–d** and $1a_H$ were performed at 298 K, while 2_I and 2_{Te} were studied at 293 K because of their higher solubility at lower temperature. (See section S3 in the SI for full details.)

ITC experiments revealed binding in 2:1 receptor–anion stoichiometry for **1a–d**, 2_I, and 2_{Te} with I^- (Table 1, Figure 2), and the same was observed in titrations of **1a** and 2_{Te} with other

DOI: 10.1021/jacs.9b00148
J. Am. Chem. Soc. 2019, 141, 4119–4129

Table 1. Equilibria and Thermodynamics of I^- Binding by XB Anion Receptors 1a–d and 2_I, ChB Receptor 2_{Te}, and HB Receptor $1a_H$ as Determined in Water by ITC[a]

	β_2 $[M]^{-2}$	K_1 $[M^{-1}]$	K_2 $[M^{-1}]$	ΔH [kJ/mol]	$T\Delta S$ [kJ/mol]
1a	1.45 (0.04) × 10^{10}	3.16 (0.06) × 10^4	4.59 (0.16) × 10^5	−52.2 (1.0)	5.9 (1.0)
1b	8.68 (2.18) × 10^9	1.60 (0.37) × 10^4	5.54 (1.32) × 10^5	−38.3 (2.1)	18.4 (2.7)
1c	1.68 (0.14) × 10^{11}	4.77 (0.40) × 10^4	3.53 (0.24) × 10^6	−55.3 (0.9)	8.8 (1.0)
1d	7.47 (0.57) × 10^6	4.87 (0.52) × 10^3	1.54 (0.11) × 10^3	−52.5 (1.8)	−13.3 (1.6)
$\mathbf{2}_{Te}$	2.64 (0.05) × 10^7	3.67 (0.41) × 10^2	7.30 (1.00) × 10^4	−31.6 (2.3)	10.1 (2.2)
$\mathbf{2}_{I}$	7.28 (0.57) × 10^9	2.87 (0.08) × 10^2	2.54 (0.22) × 10^7	−34.6 (1.4)	20.8 (1.6)
$\mathbf{1a}_H$	[b]	3.88 (0.02) × 10^3	[b]	−23.2 (0.1)	2.7 (0.1)

[a]Uncertainties are given in parentheses. All experiments were performed in unbuffered water, and I^- was introduced as NaI. Titrations were conducted at 298 K for **1a–d** and $\mathbf{1a}_H$ or at 293 K for $\mathbf{2}_{Te}$ and $\mathbf{2}_I$. [b]1:1 binding stoichiometry.

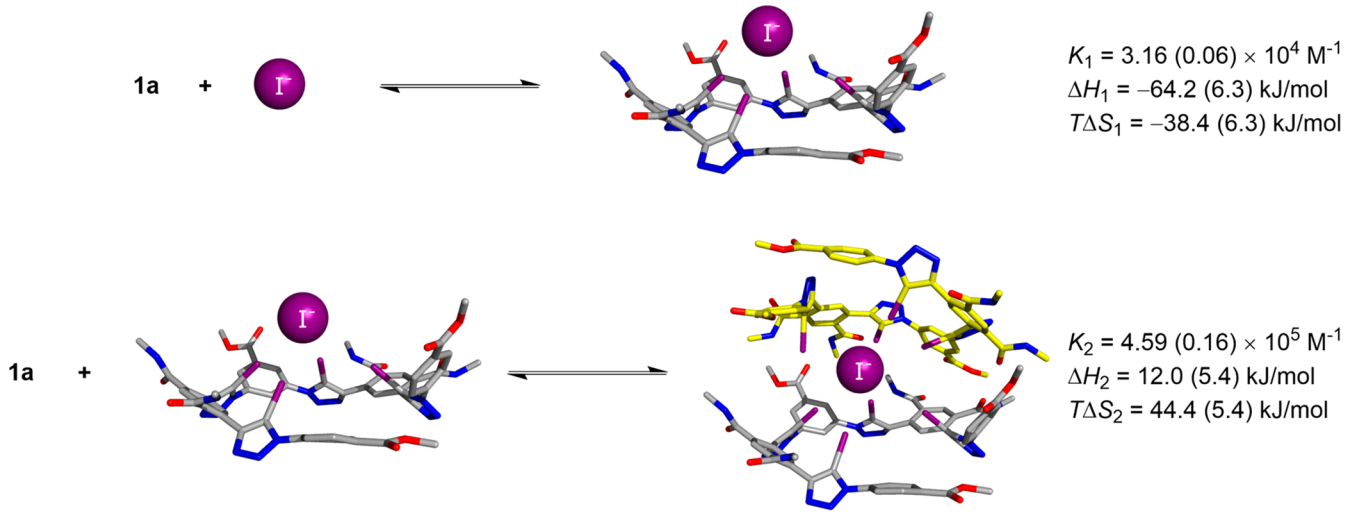

Figure 2. Equilibria and thermodynamic signatures of stepwise 2:1 binding between **1a** and I^-. The receptor model is shown with truncated solubilizing chains.

Table 2. Affinities of 1a, 2_{Te}, and $1a_H$ for a Range of Anions Determined in Water by ITC[a]

host	guest	β_2 $[M^{-2}]$[b]	K_1 $[M^{-1}]$	K_2 $[M^{-1}]$	ΔH [kJ/mol]	$T\Delta S$ [kJ/mol]
1a	NaI	1.45 (0.04) × 10^{10}	3.16 (0.06) × 10^4	4.59 (0.16) × 10^5	−52.2 (1.0)	5.9 (1.0)
	NaBr	3.43 (0.50) × 10^6	1.03 (0.13) × 10^3	3.34 (0.45) × 10^3	−25.6 (1.1)	11.7 (1.4)
	NaCl	wb	wb	wb	wb	wb
	$NaReO_4$	6.66 (0.67) × 10^8	4.91 (0.22) × 10^4	1.35 (0.08) × 10^4	−20.3 (0.5)	30.1 (0.3)
	NaSCN	3.40 (0.17) × 10^7	5.38 (0.22) × 10^3	6.33 (0.55) × 10^3	−31.0 (0.9)	12.1 (0.8)
	$NaClO_4$	1.21 (0.14) × 10^5	5.55 (0.74) × 10^1	2.19 (0.09) × 10^3	−29.4 (3.2)	−0.4 (3.4)
$\mathbf{2}_{Te}$	NaI	2.64 (0.05) × 10^7	3.67 (0.41) × 10^2	7.30 (1.00) × 10^4	−31.6 (2.3)	10.1 (2.2)
	NaBr	1.26 (0.70) × 10^3	1.69 (0.55) × 10^2	6.94 (1.56) × 10°	−13.9 (6.0)	3.2 (6.8)
	NaCl	wb	wb	wb	wb	wb
	$NaReO_4$	1.58 (0.11) × 10^6	1.84 (0.18) × 10^2	8.67 (1.09) × 10^3	−25.4 (2.5)	9.4 (2.5)
	NaSCN	5.70 (0.25) × 10^6	4.92 (0.12) × 10^2	1.16 (0.05) × 10^4	−2.0 (0.5)	35.9 (0.5)
	$NaClO_4$	wb	wb	wb	wb	wb
$\mathbf{1a}_H$	NaI		3876 (21)		−23.2 (0.1)	−2.7 (0.1)
	NaBr		[c]		[c]	[c]
	NaCl		3367 (983)		−0.5 (0.1)	19.7 (0.7)
	$NaReO_4$		wb		wb	wb
	NaSCN		346 (14)		−21.7 (0.5)	−7.2 (0.6)
	$NaClO_4$		2000 (14)		−23.3 (0.1)	−4.5 (0.1)

[a]wb, weak binding (too weak to quantify). Uncertainties are given in parentheses. All experiments were conducted in unbuffered water at 298 K for **1a** and $\mathbf{1a}_H$ or at 293 K for $\mathbf{2}_{Te}$. [b]Association constants of the 2:1 host–guest complex. [c]No satisfactory 1:1 fit was obtained, with possible complex binding equilibria.

anions (Table 2). In contrast, HB receptor $\mathbf{1a}_H$ was found to bind exclusively in 1:1 stoichiometry. This can be explained by the differences in the steric bulk of HB and σ-hole donor atoms. In the case of $\mathbf{1a}_H$, the anion guest can be bound in the plane of the folded receptor backbone in a fashion similar to that of the known triazolophane[61,62] and foldamer[63,64] examples. In XB and ChB receptors, the very large size of convergent I or MeTe units sterically forces the coordinated anion to be held above

DOI: 10.1021/jacs.9b00148
J. Am. Chem. Soc. 2019, 141, 4119–4129

the plane of the receptor. This results in a capped binding geometry as we have previously observed in the solid-state structure of a tetradentate receptor NaI complex,[53] which facilitates the coordination of a second receptor molecule to the anion. Additionally, the hydrophobic character of the σ-hole donor atoms can be expected to augment the hydrophobicity of the phenylene-triazole backbone and favor aggregation in water. Molecular dynamics simulations of the 2:1 complex of **1a** and I^- in different binding conformations (vide infra) show these structures to be stable in aqueous solution. Further evidence for the 2:1 binding mode was obtained by diffusion-ordered NMR (DOSY), which showed a decrease in diffusion coefficients upon guest addition where significant 2:1 binding was indicated by ITC. (See section S4 in the SI for more details.)

The ITC binding data for all receptors with I^- in water are collected in Table 1. XB receptors **1a**–**d** displayed very high I^- affinity, with 2:1 cumulative association constants (β_2) of up to 1.68×10^{11} M^{-2} in the case of **1c**. K_2 was 1 to 2 orders of magnitude higher than K_1 in **1a**–**c**, indicating a strong preference for 2:1 binding. In **1d**, K_2 was much lower in magnitude, which is likely due to the large size of its termini sterically disfavoring the formation of the 2:1 stoichiometric complex. Although all-ester XB receptor $\mathbf{2_I}$ displayed a β_2 value similar to that for **1a**, its binding was much more dominated by K_2. This may be attributed to the all-ester outer rim of $\mathbf{2_I}$ being relatively less hydrophilic than the mixed ester–amide functionalities of **1a**. This can be expected to disfavor the folding of $\mathbf{2_I}$ into a 1:1 binding conformation but to enhance the hydrophobic collapse into a 2:1 complex. Additionally, the higher entropic contributions in $\mathbf{2_I}$ and $\mathbf{2_{Te}}$ can be explained by the release of water molecules weakly interacting with their ester groups. It is especially noteworthy that all σ-hole–donor receptors exhibit a higher iodide binding affinity than the Na^+/I^- symporter protein (NIS, $K_a = 4.46 \times 10^4$ M^{-1}) responsible for the uptake of I^- into the follicular cells of the thyroid gland in the first step of the thyroid hormone biosynthesis.[52]

In all XB and ChB receptors, I^- binding was mainly enthalpy-driven with an overall ΔH of 2:1 binding in the range of −30 to −55 kJ/mol and generally favorable but less dominant entropic contributions. The strong exothermicity may be attributed to two effects: the ability of the σ-hole donors to form strong XB/ChB interactions with I^- within the largely dehydrated core of the host complex and the formation of HB interactions between the released water molecules and the bulk solvent.

As shown in Figure 2 for **1a**, the stepwise binding consists of the enthalpy-driven formation of the 1:1 complex followed by the entropy-driven coordination of another receptor molecule. In the first binding event, the highly exothermic signature is likely due to four strong halogen bonds being formed while the capped complex geometry allows I^- to remain significantly hydrated. In the second equilibrium formation of new XB is probably less efficient. (As shown by molecular modeling, at least six out of the eight iodotriazoles in the 2:1 complex forms XB contacts.) This binding event must therefore be driven by the favorable entropy change associated with the nearly complete dehydration of I^- and the partial dehydration of the receptor molecules. Similar thermodynamic signatures were observed for $\mathbf{2_I}$ and $\mathbf{2_{Te}}$ (Table S3-1).

Among **1a**–**d**, the unusually low enthalpic contribution seen for **1b** is an indication that XB contacts from its outer iodotriazoles are disrupted by the steric bulk of its naphthaleneimide termini. At the same time, the restricted rotation of these termini relative to the iodotriazoles is a likely explanation of the higher $T\Delta S$. In contrast, in **1d** the I^- binding is unusually entropically disfavored, which may be attributed to the loss of additional degrees of freedom in its exceptionally large termini.

ChB receptor $\mathbf{2_{Te}}$ displayed a similar binding pattern to $\mathbf{2_I}$, albeit with a much lower K_2. This indicates that the formation of a 2:1 complex by $\mathbf{2_{Te}}$ is disfavored by the additional steric bulk of Te-bound CH_3 groups. Because the K_1 and ΔH values are similar in $\mathbf{2_{Te}}$ and $\mathbf{2_I}$, it follows that the XB and ChB interactions with I^- must be of comparable strength and enthalpically driven character. The involvement of ChB in I^- coordination was confirmed by the large downfield changes in ^{125}Te chemical shifts ($\Delta\delta$) upon titration with TBAI in CD_3CN (Figure 3). In this organic solvent, $\mathbf{2_{Te}}$ formed a 1:1 binding

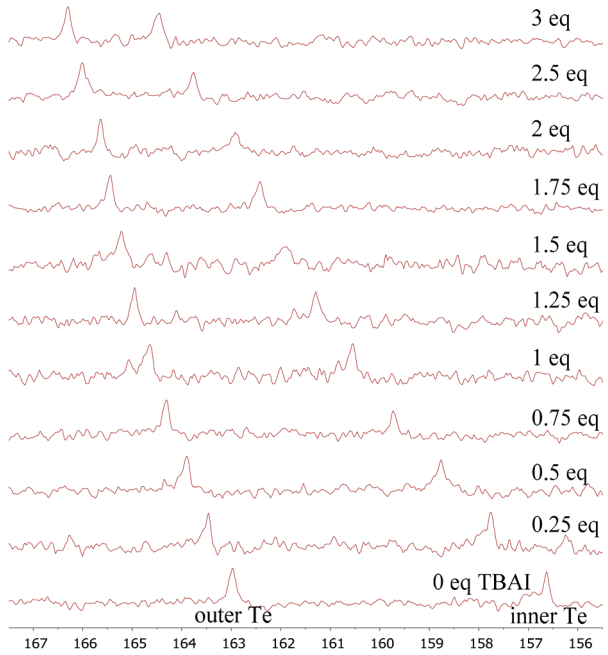

Figure 3. Changes in the ^{125}Te chemical shifts of $\mathbf{2_{Te}}$ (5 mM in CD_3CN, 298 K, 158 MHz) titrated with tetrabutylammonium iodide (TBAI).

complex with I^- ($K_a = 96.8 \pm 0.6$ M^{-1}). Combined with a smaller $\Delta\delta$ magnitude of outer Te atoms relative to the inner Te donors, this implies that in CD_3CN there is no solvophobic effect to drive the folding and 2:1 association of $\mathbf{2_{Te}}$. In water, however, hydrophobic collapse stabilizes the 1:1 and especially 2:1 bound states, prevailing over the weak solvation of I^-.

The behavior of $\mathbf{1a_H}$ is in stark contrast to that of its σ-hole counterparts. Its 1:1 I^- binding constant is lower than K_1 of **1a**–**d**, indicating a significantly weaker interaction than in XB receptors and a size mismatch with I^-. Because of its inability to form a 2:1 complex (see DOSY data in section S4 in the SI), $\mathbf{1a_H}$ has a much lower overall I^- affinity than any of the XB/ChB receptors. Similar to the σ-hole receptors, $\mathbf{1a_H}$ displays enthalpy-dominated binding, ostensibly due to the formation of weak C–H hydrogen bonding interactions with the bound I^- akin to that observed by Flood and co-workers.[50]

The exceptionally strong I^- binding by **1a** and $\mathbf{2_{Te}}$ prompted us to investigate their affinities toward a range of other anions in water by ITC. As shown in Table 2, σ-hole receptors **1a** and $\mathbf{2_{Te}}$ displayed a general preference for binding weakly hydrated anions such as SCN^- and ReO_4^- in 2:1 stoichiometry resulting

DOI: 10.1021/jacs.9b00148
J. Am. Chem. Soc. 2019, 141, 4119–4129

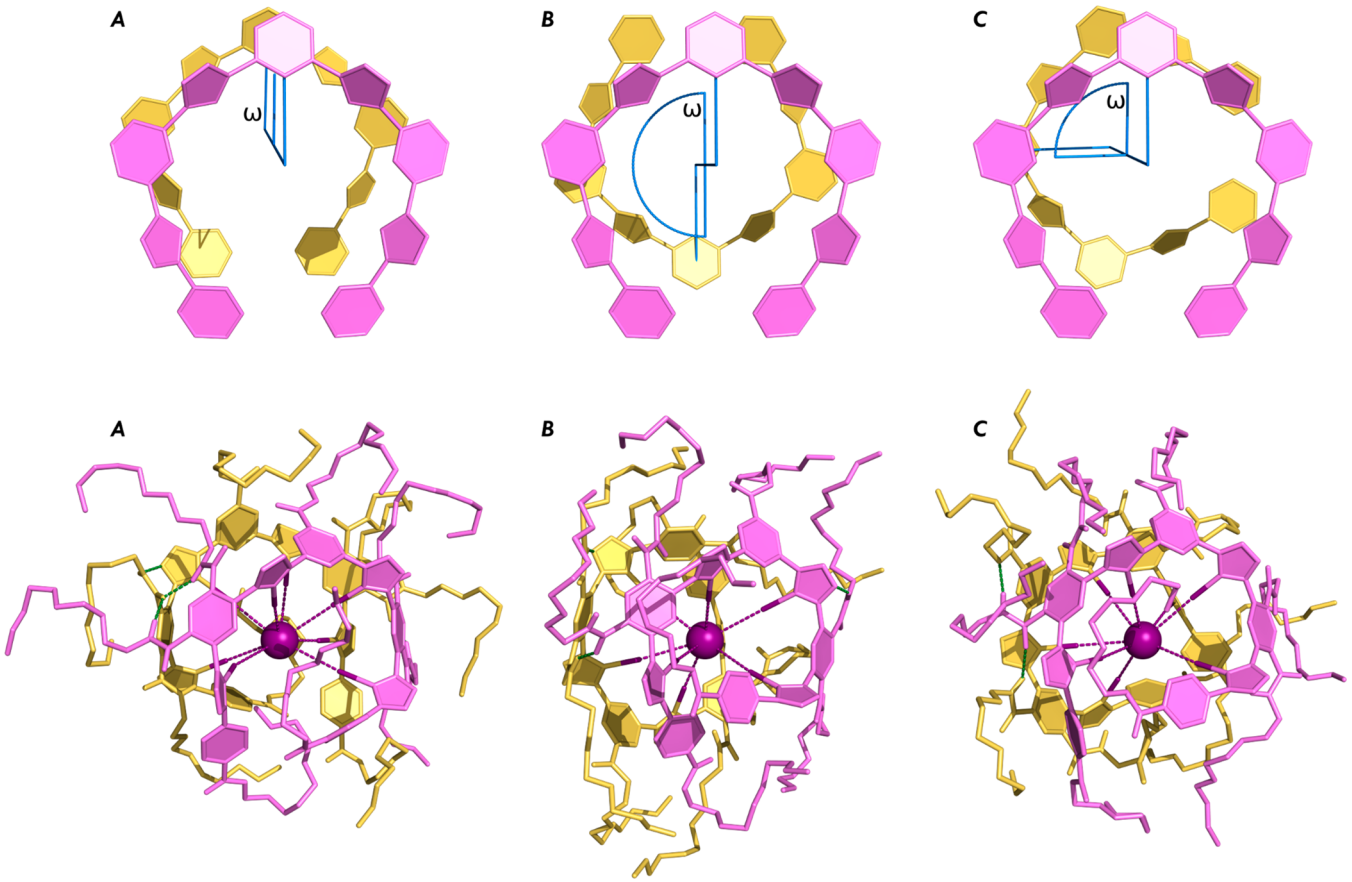

Figure 4. (Top) Sketches of binding arrangements A, B, and C in 2:1 host–guest complexes showing the ω torsion angle, defined by the centroids of the α rings and of the four triazole binding units of each foldamer. (Bottom) MM structures of 2:1 complexes $(\mathbf{1a})_2 \bullet \mathbf{I}^-$ in binding arrangements A, B, and C. The XB and HB interactions are shown by purple and green dashed lines, respectively.

from the hydrophobic collapse. On the other hand, no measurable interaction was found with ClO_3^-, NO_3^-, AcO^-, $H_2PO_4^-$, and SO_4^{2-}. In **1a**, a high selectivity for I^- (ΔH_{hyd} = −325 kJ/mol) over SCN^- and ClO_4^- (ΔH_{hyd} = −310, −229 kJ/mol, respectively)[65] indicates that shape and size complementarity effects are present. In particular, the isotropic spherical geometry of I^- likely allows maximal interactions with the highly directional σ-holes. Chalcogen bonding $\mathbf{2_{Te}}$ was also I^--selective, although the degree of discrimination over SCN^- was less pronounced. This significant I^- selectivity is in contrast to the known macrocyclic receptors with hydrophobic C–H HB donor cavities. For instance, Sindelar's water-soluble bambus[6]uril[22] preferentially binds ClO_4^- over I^-, while Pittelkow's biotin[6]uril[23] is selective for SCN^-. Likewise, in Gibb's cavitand[66] I^- binding is over an order of magnitude weaker than that of ReO_4^- and ClO_4^-. Importantly, this highlights the overriding role of σ-hole interactions in I^- recognition by **1a** and $\mathbf{2_{Te}}$.

Further evidence of the influence of σ-holes can be seen in comparison with $\mathbf{1a_H}$, which exhibits a weaker and less selective anion binding ability. Being modestly selective for I^-, it displays a surprisingly high affinity for the more hydrophilic Cl^-. Interestingly, ReO_4^- was bound strongly only by **1a** and $\mathbf{2_{Te}}$ and not $\mathbf{1a_H}$, possibly implying an intrinsic σ-hole preference for the oxoanion and better size complementarity with the XB/ChB anion binding site.[48,67,68]

All ITC experiments presented in Tables 1 and 2 were carried out in unbuffered water, as all anions of interest are pH-independent at pH >3. Likewise, the receptors do not contain significantly acidic or basic functions; in particular, the basicity of 1,2,3-triazoles is known to be very weak.[69] Additional titrations done in buffered solutions (Table S3-2) revealed almost unchanged I^- binding by **1c** at pH 4 (citrate buffer, β_2 = 2.22(0.33) × 10^{11}) and pH 7.5 (HEPES buffer, β_2 = 2.88(0.87) × 10^{11}). Small increases in affinity can be attributed to ionic strength rather than pH effects. In pH 10 $NaHCO_3/Na_2CO_3$ buffer, the binding was slightly weakened (β_2 = 3.65(0.12) × 10^{10}), which indicates possible competition from HCO_3^- or OH^- ions. Additionally, no cation influence was observed in an experiment using CsI rather than NaI (β_2 = 1.49(0.25) × 10^{11}). This confirms the expected lack of alkali metal binding sites in the receptor structure.

Computational Studies. Further structural insights into the 2:1 host–iodide stoichiometric complexes of **1a** and $\mathbf{2_{Te}}$ in water were obtained by molecular dynamics (MD) simulations, carried out using the AMBER software package[70] and the General AMBER Force Field (GAFF).[71,72] In addition, for the $\mathbf{2_{Te}}$ receptor, force field bonding parameters were developed for the tellurium center. The multiple XB and ChB interactions were described by resorting to extra points of charge following the modeling approach reported in our previous works.[46,47,49,73−77] The modeling details are thoroughly described in section S7 of the SI.

The starting binding arrangements of 2:1 host–guest complexes of **1a** and $\mathbf{2_{Te}}$ were generated as follows: two receptor molecules were superimposed with the formation of a

DOI: 10.1021/jacs.9b00148
J. Am. Chem. Soc. 2019, 141, 4119−4129

binding pocket, in which one iodide was inserted almost equidistant from the eight convergent binding units. In addition, initial binding arrangements A, B, and C, differing in the relative spatial disposition of the central phenylene rings of the two individual receptors (α phenyl rings), were considered, as depicted in Figure 4. These three ideal binding arrangements are characterized by the ω torsion angle between the centroids of the α phenyl rings and the axis defined by the centroids of the four triazole rings of each receptor. In A and B, the α phenyl rings of the two monomers are face to face and opposite to each other, leading to ω torsion angles of 0 and 180°, respectively, while intermediate arrangement C has an ω angle of 90°. Afterward, the A, B, and C binding arrangements of **1a** and $\mathbf{2}_{Te}$ structures were subject to preliminary conformational analyses at high temperature by MD simulations in the gas phase, as detailed in the SI. For both host–guest systems, three molecular mechanics (MM) energy-minimized structures were selected and are shown in Figure 4 for **1a** and in Figure S7-1 for $\mathbf{2}_{Te}$.

The values for the ω angle in the gas-phase MM minimized structures of **1a** are 20.6° (A), 172.2° (B), and 69.6° (C), while in $\mathbf{2}_{Te}$ these values are 44.8° (A), 146.1° (B), and 95.4° (C). Moreover, the seven peripheral PEG side chains of each monomer are folded around the capsule core and consequently hamper the eventual access of water molecules to the binding pocket. Thus, iodide recognition was also investigated by stretching the PEG side chains of **1a** and $\mathbf{2}_{Te}$ in the three starting arrangements. Ultimately, two alternative scenarios for the A, B, and C spatial dispositions, with folded and unfolded PEG side chains, were afforded and appointed for subsequent MD simulations carried out under periodic boundary conditions in cubic boxes with 11 500 TIP3P water molecules. Foldamer capsules **1a** and $\mathbf{2}_{Te}$ were simulated along three independent runs of 100 ns each, leading to a total of ($3 \times 2 \times 3 \times 100 =$) 1.8 μs of MD simulation for each host. Notably, along the equilibration period the unfolded PEG side chains have refolded, adopting equivalent dispositions to the ones observed in the gas phase. Consequently, the sampling data of six independent MD runs for the A, B, and C binding arrangements of **1a** and $\mathbf{2}_{Te}$ are treated together.

It is noteworthy that the dimeric capsules of **1a** and $\mathbf{2}_{Te}$ are maintained throughout the simulation time, with the iodide guest kept inside of the binding pocket, as illustrated in Figure 5 for binding arrangement A of both complexes. Equivalent depictions are presented in Figures S7-2 and S7-3 for the B and C scenarios of these dimeric receptor iodide complexes. The numbers and average dimensions of the XB and ChB interactions are summarized in Table 3. Receptor **1a** binds I^- with ca. 7 intermittent XB interactions for arrangements A and C or 6 for arrangement B. These results indicate that at least six of the eight putative XB binding units recognize the iodide during the course of the simulation time. The dimensions of the XB interactions are indistinguishable between binding arrangements, with C_{trz}–I···I^- (trz = triazole) angles roughly linear and I···I^- distances of ca. 4.0 Å, showing that the iodide guest is tightly bonded to the capsule. In addition, up to 14 N–H···O and N–H···N_{trz} hydrogen bonds between receptor molecules were intermittently observed, also assisting the maintenance of the capsular architecture (Table S7-1). In agreement with these synergetic noncovalent interactions, the three binding arrangements preserve the initial orientations, as indicated by the average ω torsion angles of 19.2 ± 9.1, 175.0 ± 5.4, and 73.3 ± 7.2° for A, B, and C, respectively.

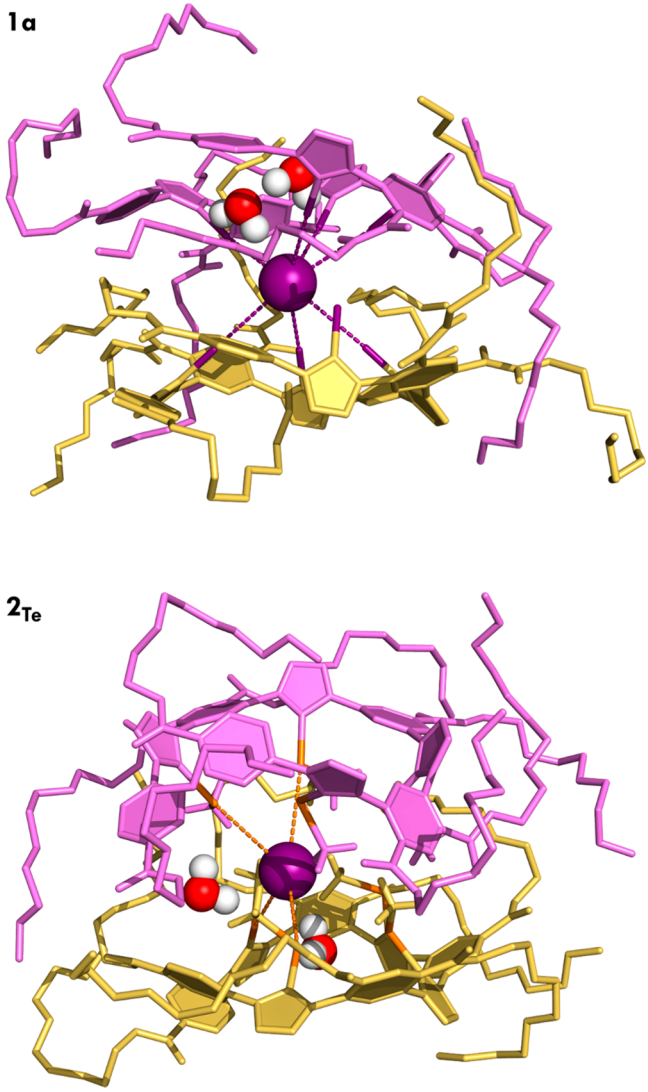

Figure 5. Representative MD snapshots of dimeric capsules of **1a** and $\mathbf{2}_{Te}$, in binding arrangement A, with the iodide guest establishing XB (purple dashed lines) or ChB (orange dashed lines) interactions with the binding units of the two foldamer entities, while being surrounded by a few water molecules.

Table 3. Average Number and Dimensions of XB or ChB Interactions for 2:1 Host–Guest Complexes of 1a and $\mathbf{2}_{Te}$ in Binding Arrangements A, B, and C[a]

host	binding arrangement	no. of XB/ChB bonds[b]	I/Te···I^- distance (Å)[b]	∠C_{trz}–I/Te···I^- (deg)[b]
1a	A	6.6 ± 0.6	4.03 ± 0.15	171.2 ± 5.9
	B	6.0 ± 0.2	3.95 ± 0.21	172.6 ± 4.1
	C	6.8 ± 0.4	4.02 ± 0.19	173.1 ± 3.6
	A + B + C	6.5 ± 0.6	4.00 ± 0.19	172.3 ± 4.7
$\mathbf{2}_{Te}$	A	5.1 ± 0.6	4.07 ± 0.15	165.5 ± 5.6
	B	5.4 ± 0.6	4.10 ± 0.17	163.7 ± 4.5
	C	4.7 ± 0.5	4.14 ± 0.17	163.9 ± 4.2
	A + B + C	5.1 ± 0.6	4.11 ± 0.17	164.3 ± 4.9

[a]Values estimated from MD simulations in water in binding arrangements A, B, and C (N = 600 000) or their concatenated data (A + B + C; N = 1 800 000). [b]XB and ChB interactions were accounted for using distances shorter than 4.5 Å and angles wider than 150°.

DOI: 10.1021/jacs.9b00148
J. Am. Chem. Soc. 2019, 141, 4119–4129

Concerning iodide binding by the $\mathbf{2}_{Te}$ capsule, the anion is shared by the eight MeTe binding units, with an average of ca. 5 ChB interactions, regardless of the binding scenario. Moreover, in spite of the similarity between the average Te···I^- and I···I^- distances (Table 3), the C_{trz}-Te···I^- angles are less linear than the C_{trz}-I···I^- angles. In addition, the weaker ChB interactions are more often interrupted than their sister XB ones within the **1a** capsule. In spite of that, the initial relative orientations between monomers in the A, B, and C binding arrangements are also preserved, with corresponding ω angles of 43.7 ± 7.8, 149.5 ± 5.1, and 89.9 ± 4.5°.

The number of water molecules residing in the capsule binding cavity of **1a** or $\mathbf{2}_{Te}$ was assessed within 5.0 Å from the guest iodide, concatenating the sampling data of the three binding arrangements. This sphere radius was selected because it roughly corresponds to the outer limit of the host binding cavity defined by the iodine or tellurium binding units. An average of 2 water molecules surrounded the encapsulated anion in both 2:1 host–guest complexes, while an MD simulation of free I^- shows that it is solvated by approximately 20 water molecules within the same 5.0 Å cutoff. In line, the radial distribution function of the water molecules around the iodide, presented in Figure S7-4, clearly shows that the dimeric foldamer capsules of **1a** and $\mathbf{2}_{Te}$ partially shelter the hosted anion from the solvent molecules at least within a 10 Å shell, as suggested by the preliminary gas-phase MM structures (Figures 4 and S7-1) and MD snapshots (Figures 5, S7-2, and S7-3). Moreover, along the MD simulations the equatorial and axial holes of the dimeric capsules are intermittently opened/closed by the flexible PEG side chains, which act as lids, limiting the access of the water molecules to the center of the binding cavity. This feature is clearly illustrated in Movie S1.

Fluorescent Anion Sensing. Compounds **1b–d** incorporate fluorophores in their termini, which are engineered to give fluorescent output upon anion binding. Compounds **1b** and **1c** showed little to no response upon titration with NaI (SI section S6). On the other hand, **1d** equipped with well-known 4-amino-1,8-naphthalene imide fluorophores[78−80] displayed a nearly 2-fold enhancement in emission intensity (Figure 6). A small hypsochromic shift in the emission maximum from 564 to 558 nm was also observed. This significant "turn-on" emission observed upon I^- addition is especially noteworthy because the "heavy atom effect" associated with this anion[81] often results in dramatic fluorescence attenuation[82] or small changes in intensity.[47,83] The main reason for the fluorescence enhancement is most likely the restriction of intramolecular motion[84] upon I^- complex formation. Although it is not clear why only **1d** exhibited a response, this may result from the increased separation of its fluorophores from the anion binding site, further reducing the quenching influence of the iodide guest.

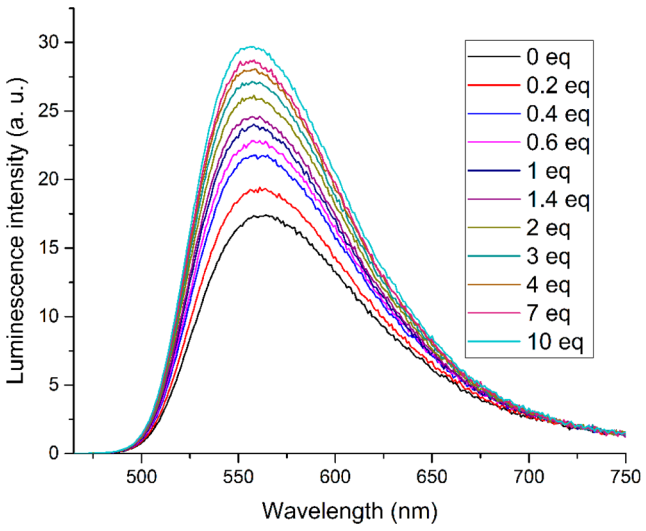

Figure 6. Luminescence spectra of **1d** (100 μM in H_2O, λ_{ex} = 442 nm) titrated with 0–10 equiv of NaI.

CONCLUSIONS

We have achieved exceptionally strong and highly selective I^- binding in pure water using unprecedented charge-neutral, non-macrocyclic XB, and ChB anion receptors. Anion binding studies in combination with molecular dynamics simulations demonstrate the formation of 2:1 receptor–I^- complexes where the I^- guest is held by multiple convergent σ-hole interactions. The hydrophobic nature of σ-hole donor atoms facilitates this folding and dimeric aggregation of receptor molecules, concomitant with the expulsion of water from the anion's hydration shell. This self-assembly of multidentate anion binding sites stabilized by hydrophobic collapse results in extremely high I^- affinity, exceeding that of the natural NIS I^- receptor by several orders of magnitude. Additionally, the use of σ-hole interactions leads to the unique selectivity for I^- over other less hydrated anions (e.g., ClO_4^-, SCN^-), which is in contrast with macrocyclic receptors containing deep hydrophobic cavities.

The binding of I^- was predominantly enthalpy-driven in all XB and ChB receptors, highlighting the formation of the respective σ-hole interactions. In the first example of a ChB anion receptor studied in water, close similarity in the properties of ChB and XB was found, as can be inferred from comparable K_1 and ΔH values in $\mathbf{2}_{Te}$ and $\mathbf{2}_I$ (Table 1). In comparison with HB analogue $\mathbf{1a}_H$, XB and ChB receptors displayed overwhelmingly higher I^- affinity and selectivity. Additionally, the introduction of fluorescent terminal groups into the XB foldamer receptor design allowed the I^- sensing capability to be demonstrated on the basis of the emission enhancement upon binding. Hence, the observations herein further champion and advance halogen and chalcogen bonding as highly effective new tools for the selective binding and sensing of anions in water. Importantly, the strategy of utilizing the hydrophobic character of σ-hole donor atoms for the self-assembly of anion binding cavities marks a paradigm shift in exploiting these interactions for anion receptor design.

ASSOCIATED CONTENT

Supporting Information

The Supporting Information is available free of charge on the ACS Publications website at DOI: 10.1021/jacs.9b00148.

Movie of a selected MD run of the 2:1 host–guest iodide complex of **1a** in binding arrangement C (AVI)

Synthesis procedures and characterization data for compounds, details of ITC and NMR anion binding studies, and computational methods (PDF)

AUTHOR INFORMATION

Corresponding Author

*paul.beer@chem.ox.ac.uk

ORCID

Arseni Borissov: 0000-0002-5408-1534

DOI: 10.1021/jacs.9b00148
J. Am. Chem. Soc. 2019, 141, 4119–4129

Igor Marques: 0000-0003-4971-9932
Jason Y. C. Lim: 0000-0002-8020-1720
Vítor Félix: 0000-0001-9380-0418
Martin D. Smith: 0000-0002-8849-488X
Paul D. Beer: 0000-0003-0810-9716

Present Address

[§]Institute of Materials Engineering and Research (IMRE), 2 Fusionopolis Way, Singapore 138634.

Notes

The authors declare no competing financial interest.

■ ACKNOWLEDGMENTS

A.B. is grateful to the EPSRC Centre for Doctoral Training in Synthesis for Biology and Medicine (EP/L015838/1) for a studentship, generously supported by AstraZeneca, Diamond Light Source, Defence Science and Technology Laboratory, Evotec, GlaxoSmithKline, Janssen, Novartis, Pfizer, Syngenta, Takeda, UCB, and Vertex. J.Y.C.L. thanks the Agency for Science, Technology and Research (A*STAR), Singapore, for postgraduate funding. V.F. acknowledges support from project PTDC/QEQ-SUP/4283/2014 (POCI-01-0145-FEDER-016895) and CICECO – Aveiro Institute of Materials (UID/CTM/50011/2013), financed by National Funds through the FCT/MEC and cofinanced by QREN-FEDER through COMPETE under the PT2020 Partnership Agreement. I.M. is grateful for a postdoctoral grant (BPD/UI98/6065/2018) under project "pAGE" (reference Centro-01-0145-FEDER-000003).

■ REFERENCES

(1) Gale, P. A.; Howe, E. N. W.; Wu, X. Anion Receptor Chemistry. *Chem.* **2016**, *1* (3), 351–422.
(2) Schmidtchen, F. P. Inclusion of Anions in Macrotricyclic Quaternary Ammonium Salts. *Angew. Chem., Int. Ed. Engl.* **1977**, *16* (10), 720–721.
(3) Lehn, J.-M. Cryptates: Inclusion Complexes of Macropolycyclic Receptor Molecules. *Pure Appl. Chem.* **1978**, *50* (9–10), 871–892.
(4) Dietrich, B.; Fyles, D. L.; Fyles, T. M.; Lehn, J.-M. Anion Coordination Chemistry: Polyguanidinium Salts as Anion Complexones. *Helv. Chim. Acta* **1979**, *62* (8), 2763–2787.
(5) Hosseini, M. W.; Lehn, J.-M. Anion receptor Molecules: Macrocyclic and Macrobicyclic Effects on Anion Binding by Polyammonium Receptor Molecules. *Helv. Chim. Acta* **1988**, *71* (4), 749–756.
(6) Alfonso, I.; Dietrich, B.; Rebolledo, F.; Gotor, V.; Lehn, J.-M. Optically Active Hexaazamacrocycles: Protonation Behavior and Chiral-Anion Recognition. *Helv. Chim. Acta* **2001**, *84* (2), 280–295.
(7) Schmidtchen, F. P.; Berger, M. Artificial Organic Host Molecules for Anions. *Chem. Rev.* **1997**, *97* (5), 1609–1646.
(8) Schmidtchen, F. P. Hosting Anions. the Energetic Perspective. *Chem. Soc. Rev.* **2010**, *39* (10), 3916–3935.
(9) Hirai, M.; Gabbaï, F. P. Squeezing Fluoride out of Water with a Neutral Bidentate Antimony(V) Lewis Acid. *Angew. Chem., Int. Ed.* **2015**, *54* (4), 1205–1209.
(10) Christianson, A. M.; Rivard, E.; Gabbaï, F. P. 1λ5-Stibaindoles as Lewis Acidic, π-Conjugated, Fluoride Anion Responsive Platforms. *Organometallics* **2017**, *36* (14), 2670–2676.
(11) Busschaert, N.; Caltagirone, C.; Van Rossom, W.; Gale, P. A. Applications of Supramolecular Anion Recognition. *Chem. Rev.* **2015**, *115* (15), 8038–8155.
(12) Ojida, A.; Mito-Oka, Y.; Inoue, M. A.; Hamachi, I. First Artificial Receptors and Chemosensors toward Phosphorylated Peptide in Aqueous Solution. *J. Am. Chem. Soc.* **2002**, *124* (22), 6256–6258.
(13) Ojida, A.; Mito-Oka, Y.; Sada, K.; Hamachi, I. Molecular Recognition and Fluorescence Sensing of Monophosphorylated Peptides in Aqueous Solution by Bis(Zinc(II)-Dipicolylamine)-Based Artificial Receptors. *J. Am. Chem. Soc.* **2004**, *126* (8), 2454–2463.
(14) Melaimi, M.; Gabbaï, F. P. A Heteronuclear Bidentate Lewis Acid as a Phosphorescent Fluoride Sensor. *J. Am. Chem. Soc.* **2005**, *127* (27), 9680–9681.
(15) Smith, D. G.; Law, G. L.; Murray, B. S.; Pal, R.; Parker, D.; Wong, K. L. Evidence for the Optical Signalling of Changes in Bicarbonate Concentration within the Mitochondrial Region of Living Cells. *Chem. Commun.* **2011**, *47* (26), 7347–7349.
(16) Liu, T.; Nonat, A.; Beyler, M.; Regueiro-Figueroa, M.; Nchiminono, K.; Jeannin, O.; Camerel, F.; Debaene, F.; Cianférani-Sanglier, S.; Tripier, R.; Platas-Iglesias, C.; Charbonnière, L. J. Supramolecular Luminescent Lanthanide Dimers for Fluoride Sequestering and Sensing. *Angew. Chem., Int. Ed.* **2014**, *53* (28), 7259–7263.
(17) Mailhot, R.; Traviss-Pollard, T.; Pal, R.; Butler, S. J. Cationic Europium Complexes for Visualizing Fluctuations in Mitochondrial ATP Levels in Living Cells. *Chem. - Eur. J.* **2018**, *24* (42), 10745–10755.
(18) Gale, P. A. Anion Receptor Chemistry. *Chem. Commun.* **2011**, *47*, 82–86.
(19) Kubik, S.; Kirchner, R.; Nolting, D.; Seidel, J. A Molecular Oyster: A Neutral Anion Receptor Containing Two Cyclopeptide Subunits with a Remarkable Sulfate Affinity in Aqueous Solution. *J. Am. Chem. Soc.* **2002**, *124* (43), 12752–12760.
(20) Schaly, A.; Belda, R.; García-España, E.; Kubik, S. Selective Recognition of Sulfate Anions by a Cyclopeptide-Derived Receptor in Aqueous Phosphate Buffer. *Org. Lett.* **2013**, *15* (24), 6238–6241.
(21) Havel, V.; Svec, J.; Wimmerova, M.; Dusek, M.; Pojarova, M.; Sindelar, V. Bambus[n]Urils: A New Family of Macrocyclic Anion Receptors. *Org. Lett.* **2011**, *13* (15), 4000–4003.
(22) Yawer, M. A.; Havel, V.; Sindelar, V. A Bambusuril Macrocycle That Binds Anions in Water with High Affinity and Selectivity. *Angew. Chem., Int. Ed.* **2015**, *54* (1), 276–279.
(23) Lisbjerg, M.; Nielsen, B. E.; Milhøj, B. O.; Sauer, S. P. A.; Pittelkow, M. Anion Binding by Biotin[6]Uril in Water. *Org. Biomol. Chem.* **2015**, *13* (2), 369–373.
(24) Lisbjerg, M.; Valkenier, H.; Jessen, B. M.; Al-Kerdi, H.; Davis, A. P.; Pittelkow, M. Biotin[6]Uril Esters: Chloride-Selective Transmembrane Anion Carriers Employing C-H···anion Interactions. *J. Am. Chem. Soc.* **2015**, *137* (15), 4948–4951.
(25) Suk, J.; Chae, M. K.; Jeong, K.-S. Indolocarbazole-Based Anion Receptors and Molecular Switches. *Pure Appl. Chem.* **2012**, *84* (4), 953–964.
(26) Politzer, P.; Murray, J. S.; Clark, T. Halogen Bonding and Other σ-Hole Interactions: A Perspective. *Phys. Chem. Chem. Phys.* **2013**, *15* (27), 11178.
(27) Cavallo, G.; Metrangolo, P.; Milani, R.; Pilati, T.; Priimagi, A.; Resnati, G.; Terraneo, G. The Halogen Bond. *Chem. Rev.* **2016**, *116* (4), 2478–2601.
(28) Lim, J. Y. C.; Beer, P. D. Sigma-Hole Interactions in Anion Recognition. *Chem.* **2018**, *4* (4), 731–783.
(29) Robertson, C. C.; Perutz, R. N.; Brammer, L.; Hunter, C. A. A Solvent-Resistant Halogen Bond. *Chem. Sci.* **2014**, *5* (11), 4179–4183.
(30) Pascoe, D. J.; Ling, K. B.; Cockroft, S. L. The Origin of Chalcogen-Bonding Interactions. *J. Am. Chem. Soc.* **2017**, *139* (42), 15160–15167.
(31) Tepper, R.; Schubert, U. S. Halogen Bonding in Solution: Anion Recognition, Templated Self-Assembly, and Organocatalysis. *Angew. Chem., Int. Ed.* **2018**, *57* (21), 6004–6016.
(32) Amendola, V.; Bergamaschi, G.; Boiocchi, M.; Fusco, N.; La Rocca, M. V.; Linati, L.; Lo Presti, E.; Mella, M.; Metrangolo, P.; Miljkovic, A. Novel Hydrogen- and Halogen-Bonding Anion Receptors Based on 3-Iodopyridinium Units. *RSC Adv.* **2016**, *6* (72), 67540–67549.
(33) Mungalpara, D.; Stegmüller, S.; Kubik, S. A Neutral Halogen Bonding Macrocyclic Anion Receptor Based on a Pseudocyclopeptide

DOI: 10.1021/jacs.9b00148
J. Am. Chem. Soc. 2019, 141, 4119–4129

with Three 5-Iodo-1,2,3-Triazole Subunits. *Chem. Commun.* **2017**, *53* (37), 5095−5098.
(34) Jungbauer, S. H.; Schindler, S.; Herdtweck, E.; Keller, S.; Huber, S. M. Multiple Multidentate Halogen Bonding in Solution, in the Solid State, and in the (Calculated) Gas Phase. *Chem. - Eur. J.* **2015**, *21* (39), 13625−13636.
(35) Jungbauer, S. H.; Huber, S. M. Cationic Multidentate Halogen-Bond Donors in Halide Abstraction Organocatalysis: Catalyst Optimization by Preorganization. *J. Am. Chem. Soc.* **2015**, *137* (37), 12110−12120.
(36) Cao, J.; Yan, X.; He, W.; Li, X.; Li, Z.; Mo, Y.; Liu, M.; Jiang, Y. B. C-I···π Halogen Bonding Driven Supramolecular Helix of Bilateral N-Amidothioureas Bearing β-Turns. *J. Am. Chem. Soc.* **2017**, *139* (19), 6605−6610.
(37) Dumele, O.; Schreib, B.; Warzok, U.; Trapp, N.; Schalley, C. A.; Diederich, F. Halogen-Bonded Supramolecular Capsules in the Solid State, in Solution, and in the Gas Phase. *Angew. Chem., Int. Ed.* **2017**, *56* (4), 1152−1157.
(38) Szell, P. M. J.; Siiskonen, A.; Catalano, L.; Cavallo, G.; Terraneo, G.; Priimagi, A.; Bryce, D. L.; Metrangolo, P. Halogen-Bond Driven Self-Assembly of Triangular Macrocycles. *New J. Chem.* **2018**, *42* (13), 10467−10471.
(39) Zapata, F.; González, L.; Caballero, A.; Bastida, A.; Bautista, D.; Molina, P. Interlocked Supramolecular Polymers Created by Combination of Halogen- and Hydrogen-Bonding Interactions through Anion-Template Self-Assembly. *J. Am. Chem. Soc.* **2018**, *140* (6), 2041−2045.
(40) Benz, S.; Macchione, M.; Verolet, Q.; Mareda, J.; Sakai, N.; Matile, S. Anion Transport with Chalcogen Bonds. *J. Am. Chem. Soc.* **2016**, *138* (29), 9093−9096.
(41) Jentzsch, A. V.; Matile, S. Transmembrane Halogen-Bonding Cascades. *J. Am. Chem. Soc.* **2013**, *135* (14), 5302−5303.
(42) Macchione, M.; Tsemperouli, M.; Goujon, A.; Mallia, A. R.; Sakai, N.; Sugihara, K.; Matile, S. Mechanosensitive Oligodithienothiophenes: Transmembrane Anion Transport Along Chalcogen-Bonding Cascades. *Helv. Chim. Acta* **2018**, *101* (4), No. e1800014.
(43) Jentzsch, A. V.; Emery, D.; Mareda, J.; Nayak, S. K.; Metrangolo, P.; Resnati, G.; Sakai, N.; Matile, S. Transmembrane Anion Transport Mediated by Halogen-Bond Donors. *Nat. Commun.* **2012**, *3*, 905.
(44) Massena, C. J.; Wageling, N. B.; Decato, D. A.; Martin Rodriguez, E.; Rose, A. M.; Berryman, O. B. A Halogen-Bond-Induced Triple Helicate Encapsulates Iodide. *Angew. Chem., Int. Ed.* **2016**, *55* (40), 12398−12402.
(45) Massena, C. J.; Decato, D. A.; Berryman, O. B. A Long-Lived Halogen-Bonding Anion Triple Helicate Accommodates Rapid Guest Exchange. *Angew. Chem., Int. Ed.* **2018**, *57* (49), 16109−16113.
(46) Langton, M. J.; Robinson, S. W.; Marques, I.; Félix, V.; Beer, P. D. Halogen Bonding in Water Results in Enhanced Anion Recognition in Acyclic and Rotaxane Hosts. *Nat. Chem.* **2014**, *6* (12), 1039−1043.
(47) Langton, M. J.; Marques, I.; Robinson, S. W.; Félix, V.; Beer, P. D. Iodide Recognition and Sensing in Water by a Halogen-Bonding Ruthenium(II)-Based Rotaxane. *Chem. - Eur. J.* **2016**, *22* (1), 185−192.
(48) Lim, J. Y. C.; Beer, P. D. Superior Perrhenate Anion Recognition in Water by a Halogen Bonding Acyclic Receptor. *Chem. Commun.* **2015**, *51* (17), 3686−3688.
(49) Lim, J. Y. C.; Marques, I.; Thompson, A. L.; Christensen, K. E.; Félix, V.; Beer, P. D. Chalcogen Bonding Macrocycles and [2]-Rotaxanes for Anion Recognition. *J. Am. Chem. Soc.* **2017**, *139* (8), 3122−3133.
(50) Hua, Y.; Liu, Y.; Chen, C. H.; Flood, A. H. Hydrophobic Collapse of Foldamer Capsules Drives Picomolar-Level Chloride Binding in Aqueous Acetonitrile Solutions. *J. Am. Chem. Soc.* **2013**, *135* (38), 14401−14412.
(51) Liu, Y.; Parks, F. C.; Zhao, W.; Flood, A. H. Sequence-Controlled Stimuli-Responsive Single-Double Helix Conversion between 1:1 and 2:2 Chloride-Foldamer Complexes. *J. Am. Chem. Soc.* **2018**, *140* (45), 15477−15486.
(52) Nicola, J. P.; Carrasco, N.; Amzel, L. M. Physiological Sodium Concentrations Enhance the Iodide Affinity of the Na+/I-Symporter. *Nat. Commun.* **2014**, *5*, 3948.
(53) Borissov, A.; Lim, J. Y. C.; Brown, A.; Christensen, K. E.; Thompson, A. L.; Smith, M. D.; Beer, P. D. Neutral Iodotriazole Foldamers as Tetradentate Halogen Bonding Anion Receptors. *Chem. Commun.* **2017**, *53* (16), 2483−2486.
(54) Hein, J. E.; Tripp, J. C.; Krasnova, L. B.; Sharpless, K. B.; Fokin, V. V. Copper(I)-Catalyzed Cycloaddition of Organic Azides and 1-Iodoalkynes. *Angew. Chem., Int. Ed.* **2009**, *48* (43), 8018−8021.
(55) Yao, T.; Larock, R. C. Regio- and Stereoselective Synthesis of Isoindolin-1-Ones via Electrophilic Cyclization. *J. Org. Chem.* **2005**, *70* (4), 1432−1437.
(56) Bubar, A.; Estey, P.; Lawson, M.; Eisler, S. Synthesis of Extended, π-Conjugated Isoindolin-1-Ones. *J. Org. Chem.* **2012**, *77* (3), 1572−1578.
(57) Stefani, H. A.; Vasconcelos, S. N. S.; Manarin, F.; Leal, D. M.; Souza, F. B.; Madureira, L. S.; Zukerman-Schpector, J.; Eberlin, M. N.; Godoi, M. N.; De Souza Galaverna, R. Synthesis of 5-Organotellanyl-1H-1,2,3-Triazoles: Functionalization of the 5-Position Scaffold by the Sonogashira Cross-Coupling Reaction. *Eur. J. Org. Chem.* **2013**, *2013* (18), 3780−3785.
(58) Potapov, V. A.; Amosova, S. V.; Khangurov, A. V.; Petrov, P. A. Synthesis of Acetylenic Tellurides by the Iodomethane-Induced Reaction of Dialkyl Ditellurides with Phenylacetylene. *Phosphorus, Sulfur Silicon Relat. Elem.* **1993**, *79*, 273−275.
(59) Hey, M. J.; Ilett, S. M.; Davidson, G. Effect of Temperature on Poly(Ethylene Oxide) Chains in Aqueous Solution. A Viscometric, 1H NMR and Raman Spectroscopic Study. *J. Chem. Soc., Faraday Trans.* **1995**, *91* (21), 3897−3900.
(60) Aroua, S.; Tiu, E. G. V.; Ishikawa, T.; Yamakoshi, Y. Well-Defined Amphiphilic C60-PEG Conjugates: Water-Soluble and Thermoresponsive Materials. *Helv. Chim. Acta* **2016**, *99* (10), 805−813.
(61) Li, Y.; Flood, A. H. Pure C-H Hydrogen Bonding to Chloride Ions: A Preorganized and Rigid Macrocyclic Receptor. *Angew. Chem., Int. Ed.* **2008**, *47* (14), 2649−2652.
(62) Hua, Y.; Ramabhadran, R. O.; Karty, J. a; Raghavachari, K.; Flood, A. H. Two Levels of Conformational Pre-Organization Consolidate Strong CH Hydrogen Bonds in Chloride-Triazolophane Complexes. *Chem. Commun.* **2011**, *47*, 5979−5981.
(63) Juwarker, H.; Lenhardt, J. M.; Pham, D. M.; Craig, S. L. 1,2,3-Triazole CH···Cl- Contacts Guide Anion Binding and Concomitant Folding in 1,4-Diaryl Triazole Oligomers. *Angew. Chem., Int. Ed.* **2008**, *47* (20), 3740−3743.
(64) Juwarker, H.; Lenhardt, J. M.; Castillo, J. C.; Zhao, E.; Krishnamurthy, S.; Jamiolkowski, R. M.; Kim, K. H.; Craig, S. L. Anion Binding of Short, Flexible Aryl Triazole Oligomers. *J. Org. Chem.* **2009**, *74* (23), 8924−8934.
(65) Smith, D. W. Ionic Hydration Enthalpies. *J. Chem. Educ.* **1977**, *54* (9), 540.
(66) Jordan, J. H.; Gibb, C. L. D.; Wishard, A.; Pham, T.; Gibb, B. C. Ion−Hydrocarbon and/or Ion−Ion Interactions: Direct and Reverse Hofmeister Effects in a Synthetic Host. *J. Am. Chem. Soc.* **2018**, *140* (11), 4092−4099.
(67) Massena, C. J.; Riel, A. M. S.; Neuhaus, G. F.; Decato, D. A.; Berryman, O. B. Solution and Solid-Phase Halogen and C-H Hydrogen Bonding to Perrhenate. *Chem. Commun.* **2015**, *51* (8), 1417−1420.
(68) Cornes, S. P.; Sambrook, M. R.; Beer, P. D. Selective Perrhenate Recognition in Pure Water by Halogen Bonding and Hydrogen Bonding Alpha-Cyclodextrin Based Receptors. *Chem. Commun.* **2017**, *53* (27), 3866−3869.
(69) Abboud, J. L. M.; Foces-Foces, C.; Notario, R.; Trifonov, R. E.; Volovodenko, A. P.; Ostrovskii, V. A.; Alkorta, I.; Elguero, J. Basicity of N-H- and N-Methyl-1,2,3-Triazoles in the Gas Phase, in Solution, and in the Solid State - An Experimental and Theoretical Study. *Eur. J. Org. Chem.* **2001**, *2001* (16), 3013−3024.

DOI: 10.1021/jacs.9b00148
J. Am. Chem. Soc. 2019, 141, 4119−4129

(70) Case, D. A.; Betz, R. M.; Botello-Smith, W.; Cerutti, D. S.; Cheatham, T. E.; Darden, T. A.; Duke, R. E.; Giese, T. J.; Gohlke, H.; Goetz, A. W.; Homeyer, N.; Izadi, S.; Janowski, P.; Kaus, J.; Kovalenko, A.; Lee, T. S. *Amber 2016*; University of California: San Francisco, CA, 2016.
(71) Wang, J.; Wolf, R. M.; Caldwell, J. W.; Kollman, P. A.; Case, D. A. Development and Testing of a General Amber Force Field. *J. Comput. Chem.* **2004**, *25* (9), 1157−1174.
(72) Wang, J.; Wolf, R. M.; Caldwell, J. W.; Kollman, P. A.; Case, D. A. Erratum: Development and Testing of a General Amber Force Field (Journal of Computational Chemistry (2004) 25 (1157)). *J. Comput. Chem.* **2005**, *26* (1), 114.
(73) Barendt, T. A.; Docker, A.; Marques, I.; Félix, V.; Beer, P. D. Selective Nitrate Recognition by a Halogen-Bonding Four-Station [3]Rotaxane Molecular Shuttle. *Angew. Chem., Int. Ed.* **2016**, *55* (37), 11069−11076.
(74) Lim, J. Y. C.; Marques, I.; Ferreira, L.; Félix, V.; Beer, P. D. Enhancing the Enantioselective Recognition and Sensing of Chiral Anions by Halogen Bonding. *Chem. Commun.* **2016**, *52* (32), 5527−5530.
(75) Lim, J. Y. C.; Marques, I.; Félix, V.; Beer, P. D. Enantioselective Anion Recognition by Chiral Halogen-Bonding [2]Rotaxanes. *J. Am. Chem. Soc.* **2017**, *139* (35), 12228−12239.
(76) Lim, J. Y. C.; Marques, I.; Félix, V.; Beer, P. D. A Chiral Halogen-Bonding [3]Rotaxane for the Recognition and Sensing of Biologically Relevant Dicarboxylate Anions. *Angew. Chem., Int. Ed.* **2018**, *57* (2), 584−588.
(77) Lim, J. Y. C.; Marques, I.; Félix, V.; Beer, P. D. Chiral Halogen and Chalcogen Bonding Receptors for Discrimination of Stereo- and Geometric Dicarboxylate Isomers in Aqueous Media. *Chem. Commun.* **2018**, *54* (77), 10851−10854.
(78) Fu, Y.; Zhang, J.; Wang, H.; Chen, J. L.; Zhao, P.; Chen, G. R.; He, X. P. Intracellular PH Sensing and Targeted Imaging of Lysosome by a Galactosyl Naphthalimide-Piperazine Probe. *Dyes Pigm.* **2016**, *133*, 372−379.
(79) Loving, G.; Imperiali, B. A Versatile Amino Acid Analogue of the Solvatochromic Fluorophore 4-N,N-Dimethylamino-1,8-Naphthalimide: A Powerful Tool for the Study of Dynamic Protein Interactions. *J. Am. Chem. Soc.* **2008**, *130* (41), 13630−13638.
(80) Kang, L.; Xing, Z. Y.; Ma, X. Y.; Liu, Y. T.; Zhang, Y. A Highly Selective Colorimetric and Fluorescent Turn-on Chemosensor for Al3+ Based on Naphthalimide Derivative. *Spectrochim. Acta, Part A* **2016**, *167*, 59−65.
(81) Basu, G.; Kubasik, M.; Anglos, D.; Secor, B.; Kuki, A. Long-Range Electronic Interactions in Peptides: The Remote Heavy Atom Effect. *J. Am. Chem. Soc.* **1990**, *112* (25), 9410−9411.
(82) Mullaney, B. R.; Thompson, A. L.; Beer, P. D. An All-Halogen Bonding Rotaxane for Selective Sensing of Halides in Aqueous Media. *Angew. Chem., Int. Ed.* **2014**, *53* (43), 11458−11462.
(83) Zapata, F.; Caballero, A.; Molina, P.; Alkorta, I.; Elguero, J. Open Bis(Triazolium) Structural Motifs as a Benchmark to Study Combined Hydrogen- and Halogen-Bonding Interactions in Oxoanion Recognition Processes. *J. Org. Chem.* **2014**, *79* (15), 6959−6969.
(84) Mei, J.; Leung, N. L. C.; Kwok, R. T. K.; Lam, J. W. Y.; Tang, B. Z. Aggregation-Induced Emission: Together We Shine, United We Soar! *Chem. Rev.* **2015**, *115* (21), 11718−11940.

DOI: 10.1021/jacs.9b00148
J. Am. Chem. Soc. 2019, 141, 4119−4129